https://doi.org/10.5194/acp-2020-754
Preprint. Discussion started: 12 August 2020

Atmospheric Chemistry and Physics Discussions

A-Train estimates of the sensitivity of warm rain likelihood and efficiency to cloud size, environmental moisture, and aerosols

Kevin M. Smalley[1] and Anita D. Rapp[1]

[1]Department of Atmospheric Sciences, Texas A&M University, College Station, Texas

Correspondence: Kevin M. Smalley (ksmalley@tamu.edu)

Abstract. Precipitation efficiency has been found to play an important role in constraining the sensitivity of the climate through its role in controlling cloud cover, yet understanding of its controls are not fully understood. Here we use CloudSat observations to identify individual contiguous shallow cumulus cloud objects and compute the ratio of cloud water path to rain water path as a proxy for warm rain efficiency (WRE). Cloud objects are then conditionally sampled by cloud-top height, relative humidity, and aerosol optical depth (AOD) to analyze changes in WRE as a function of cloud size (extent). For a fixed cloud-top height, WRE increases with extent and environmental humidity following a double power-law distribution, as a function of extent. Similarly, WRE increases holding environmental moisture constant. There is surprisingly little relationship between WRE and AOD when conditioned by cloud-top height, suggesting that once rain drop formation begins, aerosols may not be as important for WRE as cloud size and depth. Consistent with prior studies, results show an increase in WRE with sea surface temperature. However, for a given depth and SST, WRE is also dependent on cloud size and becomes larger as cloud size increases. Given that larger objects become more frequent with increasing SST, these results imply that increasing precipitation efficiencies with SST are due not only to deeper clouds with greater cloud water contents, but also the propensity for larger clouds which may have more protected updrafts.

1 Introduction

Low cloud cover continues to be a dominant source of uncertainty in projecting future climate (e.g. Bony and Dufresne, 2005; Dufresne and Bony, 2008; Vial et al., 2013), with variations in shallow cumulus distributions explaining much of the differences in climate model-derived estimates of climate sensitivity (e.g. Wyant et al., 2006; Medeiros and Stevens, 2011; Nam et al., 2012). This stems from climate models' inability to simulate shallow cumulus and their impacts, due in part to the low temporal and spatial resolution of these models (e.g. Stevens et al., 2002), as well as the fact that small-scale processes important for cloud development, including turbulence and convection, must be parameterized (e.g. Tiedtke, 1989; Zhang and McFarlane, 1995; Bretherton et al., 2004). Studies have shown precipitation efficiency is a key parameter used to constrain cloud parameterizations within climate models (Rennó et al., 1994; Del Genio et al., 2005; Zhao, 2014; Lutsko and Cronin,

https://doi.org/10.5194/acp-2020-754
Preprint. Discussion started: 12 August 2020


Atmospheric Chemistry and Physics Discussions

2018). Nam et al. (2012) hypothesized that shallow cumulus are too reflective in climate models, possibly because model precipitation efficiencies are too weak. This results in excess cloud water which increases cloud optical depth and shallow cumulus reflectance. Prior observational and modeling studies found the precipitation efficiency of shallow cumulus increases as sea-surface temperature (SST) increases in response to climate change (Lau and Wu, 2003; Bailey et al., 2015; Lutsko and Cronin, 2018). Factors including environmental moisture (e.g. Heus and Jonker, 2008; Schmeissner et al., 2015), entrainment (e.g. Korolev et al., 2016; Pinsky et al., 2016b, a), and aerosols (e.g. Koren et al., 2014; Dagan et al., 2016; Jung et al., 2016b, a) help regulate both thermodynamic and dynamical processes that promote favorable conditions important to not only warm rain production, but also the efficiency of the conversion of cloud water to precipitation. To better constrain cloud parameterizations of these processes and subsequently climate sensitivity to low cloud cover, more observations-based studies analyzing physical processes influencing warm rain efficiencies are needed.

In an ideal shallow cumulus cloud, liquid water content increases adiabatically from cloud base to top. However, liquid water content is generally only 50% - 80% of the adiabatic values due to entrainment (Gerber et al., 2008). Evaporation induced by cloud-edge mixing not only impacts shallow cumulus updraft strength, but also the number and size of droplets within a cloud (Lu et al., 2012), with increased evaporation potentially reducing the number and size of available droplets. Using a large-eddy simulation (LES), Moser and Lasher-Trapp (2017) found the influence of entrainment decreases from cloud-edge to center of individual shallow cumulus as they grow larger. This results in liquid water content at cloud center being closer to adiabatic in larger clouds, because fewer droplets evaporate away at cloud-center. This implies that the collision-coalescence process is more efficient at cloud center, because there is more cloud water available to be collected by large droplets. At cloud edge, there are not only fewer droplets but also smaller droplets, potentially reducing collision-coalescence efficiencies there. This is consistent with other LES results that found shallow cumulus updrafts are more insulated from entrainment as they increase in size (e.g. Heus and Jonker, 2008; Burnet and Brenguier, 2010; Tian and Kuang, 2016). LES and limited field-campaign observational studies have shown that cloud updrafts not only become more protected as cloud size increases, but also as environmental moisture increases (Heus and Jonker, 2008; Schmeissner et al., 2015; Hernandez-Deckers and Sherwood, 2018). Romps (2014) used a cloud model to show that precipitation efficiency decreases as relative humidity decreases, because precipitation evaporates more readily in a drier environment. Considering environmental moisture scales with temperature, this is consistent with results found by Lau and Wu (2003) which show the efficiency of warm rain production increases as SSTs increase using Tropical Rainfall Measuring Mission (TRMM) satellite observations. Given LES results showing that shallow cumulus updrafts are more protected as clouds grow in size and/or environmental moisture increases, *we hypothesize larger droplets will be evident closer to the cloud base and increase WRE in larger cloud objects, because the cloud-core of larger cloud objects is more protected from entrainment*.

While perhaps not as important as organization (Minor et al., 2011) or cloud size (Jiang and Feingold, 2006), it is widely understood that aerosol concentrations act to suppress warm rain production (Twomey, 1974; Albrecht, 1989) by increasing the cloud droplet concentration and reducing cloud droplet sizes (Squires, 1958). Albrecht (1989) found that increasing precipitation efficiency within a model is equivalent to decreasing the amount of cloud concentration nuclei (CCN), which reduces the amount of cloud water. Similarly, Saleeby et al. (2015) used a cloud model to recently find both cloud water and rain drop

https://doi.org/10.5194/acp-2020-754
Preprint. Discussion started: 12 August 2020


Atmospheric Chemistry and Physics Discussions

concentration decreases as cloud concentration nuclei increases. Lebsock et al. (2011) used CloudSat and Moderate Resolution Imaging Spectroradiometer (MODIS) observations to show that as drop size decreases, the ratio of rain water to cloud water also decreases. Together, these studies suggest the number of large droplets able to fall at sufficient terminal velocities to initiate collision-coalescence and continue growing to large enough sizes to fall out as rain decreases with increasing aerosol concentrations, which would reduce warm rain efficiency (WRE).

Observationally, prior studies have used satellite observations to infer the relationship between precipitation efficiency and both sea-surface temperature (Lau and Wu, 2003) and drop size (Lebsock et al., 2011). However, the relationship between cloud water and precipitation as shallow cumulus grow larger, environmental moisture increases, and/or aerosol loading has only been investigated using cloud models (e.g. Moser and Lasher-Trapp, 2017) and limited field-campaign observations (e.g. Gerber et al., 2008). While these case and model studies provide insight into the physical processes, it is unclear how well they represent the shallow cumulus clouds observed globally. Satellites can observe a large enough sample size of shallow cumulus over different regions and during different stages of their lifecycle to gain a more holistic view of this relationship. Prior studies have used TRMM and Global Precipitation Measurement Mission (GPM) observations to analyze warm rain production and efficiency (e.g. Lau and Wu, 2003). Unfortunately, TRMM and GPM are precipitation radars operating at the Ku- and Ka-bands not capable of observing the non-raining portions of clouds or light precipitation. Building off work in Smalley and Rapp (2020) that analyzed the relationship between rain likelihood and cloud size, this study uses the higher sensitivity radar of CloudSat in addition to MODIS observations to test the hypothesis that *WRE is higher in larger shallow cumulus and is modulated by environmental moisture and aerosol loading*.

2 Data and Methods

To determine if larger shallow cumulus clouds are more efficient at producing warm rainfall, this study uses the CloudSat Cloud Profiling Radar (CPR; Tanelli et al., 2008) to identify individual contiguous shallow cumulus cloud objects. The CPR is a near-nadir pointing 94-GHz radar that can observe raining and non-raining cloud drops. It allows us to analyze the horizontal distribution of cloud within a horizontal footprint of 1.4 x 1.8 km, and the vertical distributions of clouds within a 240 m bin within each cloudsat pixel.

Contiguous cloudy regions are initially identified using the 2B-GEOPROF (Marchand et al., 2008) cloud mask confidence values ≥ 20, which removes orbit elements that may be influenced by ground clutter (Marchand et al., 2008). Before identifying cloud objects, 2C-RAIN-PROFILE (Lebsock and L'Ecuyer, 2011) modeled reflectivity is mapped onto the two-dimensional cloud mask field. As outlined by prior literature (e.g. L'Ecuyer and Stephens, 2002; Mitrescu et al., 2010; Lebsock and L'Ecuyer, 2011), modeled reflectivity adjusts the raw reflectivity for multi-scattering and attenuation when it is raining. As described by Smalley and Rapp (2020), we use a lower-tropospheric stability threshold of 18.55 K to separate cloud objects occurring in environments favoring stratocumulus development from those occurring in environments favoring shallow cumulus development. Shallow cumulus cloud objects are then identified using the methodology described by Smalley and Rapp (2020) using the combined two-dimensional reflectivity field, with only single-layer cloud objects included. This study uses

https://doi.org/10.5194/acp-2020-754
Preprint. Discussion started: 12 August 2020


Atmospheric Chemistry and Physics Discussions

2C-RAIN-PROFILE integrated precipitation water path path (W_P) > 0 to identify raining cloud objects and does not consider non-raining objects. We then store the median cloud-top height and maximum along-track extent (hereby extent) of each cloud object for later analysis.

Although CloudSat 2B-CWC-RVOD (Austin et al., 2009) does provide a cloud water path (W_C) product, the rain drop size distribution used in 2B-CWC-RVOD is not the same as that used in 2C-RAIN-PROFILE. Additionally, Christensen et al. (2013) found that the 2B-CWC-RVOD algorithm struggles to filter out precipitation sized droplets in the presence of light precipitation and drizzle, which results in an overestimation of cloud water. This, coupled with differences in assumed drop size distributions by 2B-CWC-RVOD and 2C-RAIN-PROFILE, makes 2B-CWC-RVOD W_C not ideal for this study, so we instead use MODIS W_C. While there are biases in MODIS shallow cumulus W_C, prior studies have found them to be small in comparison to other satellite retrievals (e.g. Lebsock and Su, 2014). W_C is then calculated for each CloudSat pixel by averaging the nearest nine MOD-06-1KM (Platnick et al., 2003) pixels, which have been previously matched to the CloudSat track in the MOD-06-1KM product (**?**). We then store and analyze the median W_C associated with each cloud object.

WRE of each shallow cumulus cloud object is calculated as $\frac{W_P}{W_C}$. Note, this is a proxy for true WRE, because mass flux of water in and out of a cloud cannot be determined without a model, however this ratio has been used by prior observational studies to analyze the amount of cloud water converted to rain water (e.g. Lebsock et al., 2011).

Considering reflectivity is a function of the drop size distribution to the sixth power, it is expected that the maximum reflectivity in non-raining cloud objects will occur near cloud-top, then shift downward as a cloud transitions from non-raining to raining. Wang et al. (2017) used the vertical reflectivity gradient (VGZ) to investigate warm rain onset. They found VGZ (positive down) reverses sign (positive to negative) when clouds transition from non-raining to raining. Given previous studies and results shown in Smalley and Rapp (2020) finding rain is more likely as clouds grow larger in extent, it is hypothesized that the negative VGZ within individual raining cloud objects will increase in magnitude as cloud objects increase in extent. The methodology developed by Wang et al. (2017) is applied to find the VGZ for each pixel within every shallow cumulus cloud object. VGZ at cloud object center pixel (VGZ_{CP}) will then be compared to VGZ at cloud object edge pixel (VGZ_{EP}) to infer the impact of mixing on cloud object cores as a function of cloud size and environmental moisture.

The influence of aerosols on the relationship between WRE and cloud object efficiency are determined using Aqua MODIS level-3 daily 550 nm aerosol optical depth (AOD) (Ruiz-Arias et al., 2013). Each cloud object is matched to the nearest 1°x1° gridbox AOD value. Note, this study does not consider the type of aerosol present in each environment, however this may also factor into the WRE.

Similar to Smalley and Rapp (2020), analysis is constrained to only marine shallow cumulus between between 60 N and 60 S. Measurements are constricted to June 2006 and December 2010 because CloudSat stopped taking night time measurements after 2010 due to a battery anomaly (Witkowski et al., 2012). Environmental moisture is classified using 6-hourly ECMWF-AUX (Cronk and Partain, 2017) average relative humidity below 3 km matched to each cloud object. Cloud-top height, environmental moisture, VGZ, and AOD are used to control and analyze the relationship between WRE and cloud object extent.

https://doi.org/10.5194/acp-2020-754
Preprint. Discussion started: 12 August 2020


Atmospheric Chemistry and Physics Discussions

3 Warm rain relationship to extent

Similar to Smalley and Rapp (2020), The spatial distribution of W_P, W_C, WRE, AOD, and extent of raining shallow cumulus cloud objects is analyzed by binning them to a 2.5° x 2.5° global grid.

Figure 1a shows the spatial distribution of W_P over the global ocean basins, with W_P increasing equatorward. This is consistent with prior literature that found raining shallow cumulus are most frequent within the tropics (e.g. Smalley and Rapp, 2020). W_P is largest near the Inter-Tropical Convergence Zone (ITCZ), South Pacific Convergence Zone (SPCZ), and tropical warm pool, with values exceeding 45 g m^{-2}. Deep convection is more frequent here (e.g. Waliser and Gautier, 1993), so some objects may be transitioning from raining shallow cumulus to deeper convection. The results likely include a mix of frequently occurring tropical raining shallow cumulus and the early stages of developing deep convection possibly resulting in large W_P over the tropics.

Spatial patterns in W_C (Figure 1b) within the tropics generally follow W_P, with values ranging between 110 g m^{-2} and 150 g m^{-2} in the tropics. Considering the tropics are more humid than the mid-latitude and polar regions, this is consistent with modeling studies that found less cloud water evaporates away in wetter environments (e.g. Hernandez-Deckers and Sherwood, 2018). Considering boundary layer depth scales with SST (e.g. Wood and Bretherton, 2004b), the boundary layer is generally deeper over the tropical oceans than the sub-tropical oceans. This supports deeper clouds (e.g. Short and Nakamura, 2000; Rauber et al., 2007; Smalley and Rapp, 2020) and could also help explain why W_C and WP are largest in the tropics.

Figure 1c shows the spatial patterns in WRE follow spatial patterns in W_P, with values increasing equatorward. Shallow cumulus cloud object WRE is largest within the ITCZ, SPCZ, and tropical warm pool, with values > 0.35. This is consistent with Lau and Wu (2003), who found precipitation efficiency is positively correlated with SST (e.g. Lau and Wu, 2003), and implies that WRE is higher in wetter environments.

Patterns in spatial extent shown in Figure 1d are similar to those found by Smalley and Rapp (2020), who used combined CloudSat/CALIPSO to define extent, with extent decreasing from the stratocumulus regions east into the trade cumulus regions and north into the ITCZ. Interestingly, Figure 1c shows WRE also peaks in the southeast Pacific stratocumulus region, implying that WRE is high in regions with relatively low SST. However, Figure 1e shows that fewer than 40 shallow cumulus objects are observed in a given gridbox over this region in a four-year period, reducing confidence in WRE here. Together, Figures 1c and 1d indicate that the relationship between WRE and extent is complicated and potentially depends on cloud depth (which increases in the tropics) and on environmental conditions including environmental moisture and aerosol loading.

To determine how WRE depends on cloud size, Figure 2 shows WRE as a function of cloud object extent. WRE follows a double power-law relationship, with WRE < 0.25 for cloud objects < 8.3 km and approaching 0.3 for cloud objects > 8.3 km. Similar to these results, earlier studies have shown a double power-law distribution in shallow cumulus size (e.g. Benner and Curry, 1998; Trivej and Stevens, 2010), which will be discussed in further detail later.

To address the impact of environmental moisture and cloud depth on WRE, Figure 3 shows the relationship between WRE and cloud object extent conditioned using cloud-top height and $<$ 3 km relative humidity. Holding environmental moisture constant, WRE depends strongly on cloud-top height with WRE nearly doubling for each 0.5km increase in cloud top height

https://doi.org/10.5194/acp-2020-754
Preprint. Discussion started: 12 August 2020


Atmospheric Chemistry and Physics Discussions

for a given extent. For a given RH and top height, there is also an increase in WRE with extent. Holding top height constant, there is also an increase in WRE with increasing environmental moisture; however, increases in WRE are dominated by changing cloud size (depth and extent).

To support the hypothesis that larger shallow cumulus are able to sustain a larger droplet field within their cores to increase the precipitation efficiency, the variation in the VGZ across individual cloud objects is examined. We expect that VGZ will be a larger negative value near cloud center than cloud edge especially as cloud size increases. As an example, Figure 4a shows the change in median VGZ_{CP} to VGZ_{EP} for cloud objects with an extent of 10.2 km. VGZ decreases from 10 dBZ km^{-1} at cloud object edge to approximately -20 dBZ km^{-1} at cloud object center. This demonstrates that larger droplets are present near cloud base near cloud object center compared to the edge. This implies, at least for extents of 10.5 km, drops grow larger near cloud object centers and may be more protected from mixing.

Figure 4b shows the relationship between VGZ_{CP} and VGZ_{EP} as a function of extent and top height. For a constant cloud-top height, VGZ_{CP} again follows a double power-law distribution. Specifically, the magnitude of the VGZ_{CP} rapidly increases from approximately 10 dBZ km^{-1} to 20 dBZ km^{-1} as extent approaches 8.3 km, while it plateaus around 20 dBZ km^{-1} for extents $>$ 8.3 km. Conversely, VGZ_{EP} decreases in magnitude, approaching 0 dBZ km^{-1} for the largest cloud object extents. However, it does not decrease as fast as VGZ_{CP}, implying that the change in vertical reflectivity gradient in the center of cloud is driving changes in differences from center to edge. Figure 4b also shows that the change in VGZ_{CP} depends on cloud-top height, with larger magnitudes for the tallest clouds. This is consistent with previous modeling studies that found larger shallow cumulus cloud cores are more insulated from entrainment (e.g. Burnet and Brenguier, 2010; Hernandez-Deckers and Sherwood, 2018), resulting in larger droplets (e.g. Moser and Lasher-Trapp, 2017) and a higher probability of rainfall (e.g. Smalley and Rapp, 2020) in observations.

To determine how VGZ_{CP} influences the relationship between WRE and extent, Figure 4c shows WRE as a function of extent conditioned by top height and VGZ_{CP}, with WRE increasing as the magnitude of VGZ_{CP} increases. This, coupled with Figure 4b, illustrates that as shallow cumulus grow deeper and wider, drops at the center of the cloud can grow larger and scavenge more available cloud water. This is consistent with larger shallow cumulus being more efficient at producing rainfall, perhaps in part because they are less influenced by environmental mixing.

Until this point, this paper has focused on how cloud size and environmental moisture impacts WRE. However, it is also understood that aerosol concentrations influence both the number and size of droplets within a cloud, with larger aerosol concentrations resulting in a greater number of smaller droplets (e.g. Twomey, 1974; Albrecht, 1989). As a result, we hypothesize increasing aerosol concentrations, which vary regionally (Figure 1f), increase the ratio of cloud droplets to rain drops, thus reducing WRE.

Figure 5a shows the relationship between WRE and AOD, conditioned by top height. On first glance, it appears that WRE increases as a function of AOD, which contradicts the expectation of a shift in drop size distribution towards fewer large drops to initiate collision-coalescence which would reduce the amount of cloud water converted to rain water. However, disentangling aerosol-cloud interactions from other meteorological variables is quite difficult, as increasing aerosol concentrations are often correlated with other environmental variables (e.g. Koren et al., 2014).

https://doi.org/10.5194/acp-2020-754
Preprint. Discussion started: 12 August 2020


Atmospheric Chemistry and Physics Discussions

Given the strong dependence of WRE on top height, we further examine the relationship between AOD and top height (Figure 5b), conditioned by extent. The curves shown in Figure 5a look similar to those shown in Figure 5b, suggesting the positive correlation between aerosols and top height are responsible for the observed relationship between AOD and WRE. Indeed, Figure 5c further supports this assertion. When conditioned by top height, WRE shows little dependence on AOD, and suggests that the conversion from W_C to W_P is more sensitive to cloud depth than aerosols. While these results seem counterintuitive, this analysis examines clouds in which precipitation has been detected. Examination of the likelihood of precipitation shows the expected decrease with increasing AOD (not shown). These results imply that once the condensation-coalescence is initiated, aerosol loading has a smaller impact on the conversion of cloud water to rain than other cloud or environmental characteristics.

4 Summary and Discussion

This study uses the methodology described by Smalley and Rapp (2020) to classify a large global shallow cumulus cloud object dataset from CloudSat and determine the relationship between WRE, cloud extent, environmental moisture, and aerosol loading. We find that WRE increases as a function of cloud size (top height and extent) and environmental moisture. Benner and Curry (1998) found a double-power law distribution in shallow cumulus thickness as a function of cloud diameter, and Trivej and Stevens (2010) hypothesized that the shift from one power-law distribution to another results from small shallow cumulus that can rapidly grow in size until reaching the trade inversion. We find a similar relationship between WRE and extent, showing that one distribution exists with WRE increasing faster for extents < 8.3 km then slowly increasing above this breakpoint. Trivej and Stevens (2010) also found that environmental factors, particularly environmental moisture, become important once cloud-top height reaches the trade inversion. Our results show that WRE is most sensitive to environmental moisture above an extent of 8.3 km, which we assume represents the average extent where cloud objects reach the trade inversion.

Unexpectedly, we find that for a fixed cloud depth, WRE is fairly insensitive to AOD. One explanation may be that, although high AOD values do occur over the global ocean basins, the majority of cloud objects being sampled still form in relatively clean air, so the minority of cloud objects occurring over polluted regions have a small impact on the overall statistics. Another explanation may be that this analysis only includes precipitating clouds, so once collision-coalescence is initiated, the amount of cloud water converted to rain water is less influenced by aerosol concentrations.

Past studies conclude that precipitation efficiency increases as SST increases (Lau and Wu, 2003; Bailey et al., 2015; Lutsko and Cronin, 2018). Considering warmer SSTs tend to result in deeper clouds (e.g. Wood and Bretherton, 2004a) and more humid environments (e.g. Chen and Liu, 2016), it is reasonable to expect that WRE would increase in response (e.g. Lau and Wu, 2003). Our results show that WRE is highest near the equator where SSTs are warmest. However, the general relationship between cloud size (depth and extent), environmental moisture, and WRE suggests that WRE is more sensitive to cloud size than environmental moisture. To directly address the SST dependence, Figure 6 shows the frequency distribution of extents and the median WRE, both as a function of cloud-top height and SST. For a given cloud-top height, WRE does increase as

https://doi.org/10.5194/acp-2020-754
Preprint. Discussion started: 12 August 2020


Atmospheric Chemistry and Physics Discussions

a function of SST. However, for a fixed SST, WRE also increases as extent increases. Additionally, Figure 6 shows that the frequency distribution of cloud object sizes shifts toward more frequent larger extents with increasing SST. Together, these suggest that increasing WRE with SST shown in past studies not only results from the deepening clouds but also the shift towards more frequent larger clouds.

Prior literature has shown that modeled shallow cumulus cores become more adiabatic as they grow larger (Moser and Lasher-Trapp, 2017), potentially resulting in larger drops. Figure 6 and our analysis of the relationship between VGZCP, extent, and WRE suggest drop growth is being enhanced near the base at the center of larger cloud objects, potentially resulting in more cloud water being scavenged by larger droplets and more efficient autoconversion and accretion processes. Most climate models parameterize autoconversion and accretion as functions of cloud and precipitation properties (e.g. Lohmann and Roeckner, 1996; Liu and Daum, 2004; Morrison et al., 2005; Lim and Hong, 2010; Lee and Baik, 2017), but recently enhancement factors that depend on variations and covariations in WC and WP have been introduced to correct for biases due to subgrid-scale Wc and Wp inhomogeneity (e.g. Lebsock et al., 2013; Boutle et al., 2014; Witte et al., 2019). Presumably, the dependence of these enhancement factors on Wc variability would capture the increase in WRE with cloud depth shown here, however it is unclear if these enhancement factors based on the variance in Wc and Wp capture the effects of cloud extent on WC and WP, and subsequently WRE. Our dataset provides an opportunity for a future analysis that could focus on investigating the relationship between subgrid-scale variability in WC, WP, WRE, and extent, which could help improve our understanding and simulation of precipitating shallow cloud processes in climate models.

Data availability. All CloudSat/MODIS data products used in this analysis were acquired from the CloudSat Data Processing Center and can be accessed at http://www.cloudsat.cira.colostate.edu.

Code and data availability. Please contact the authors for access to any dataset created by the analysis and/or the code used to process the CloudSat/MODIS data..

Author contributions. Kevin Smalley performed the analysis. While, Kevin Smalley and Anita Rapp wrote and edited this manuscript.

Competing interests. The authors declare they have no conflicts of interest.

Acknowledgements. This research was supported by NASA grant NNX14AO72G.

https://doi.org/10.5194/acp-2020-754
Preprint. Discussion started: 12 August 2020

Atmospheric Chemistry and Physics Discussions

References

Albrecht, B. A.: Aerosols, Cloud Microphysics, and Fractional Cloudiness, Science, 245, 1227–1230, https://doi.org/10.1126/science.245.4923.1227, https://science.sciencemag.org/content/245/4923/1227, 1989.

Austin, R. T., Heymsfield, A. J., and Stephens, G. L.: Retrieval of ice cloud microphysical parameters using the CloudSat millimeter-wave radar and temperature, Journal of Geophysical Research: Atmospheres, 114, https://doi.org/10.1029/2008JD010049, https://agupubs.onlinelibrary.wiley.com/doi/abs/10.1029/2008JD010049, 2009.

Bailey, A., Nusbaumer, J., and Noone, D.: Precipitation efficiency derived from isotope ratios in water vapor distinguishes dynamical and microphysical influences on subtropical atmospheric constituents, Journal of Geophysical Research: Atmospheres, 120, 9119–9137, https://doi.org/10.1002/2015JD023403, https://agupubs.onlinelibrary.wiley.com/doi/abs/10.1002/2015JD023403, 2015.

Benner, T. C. and Curry, J. A.: Characteristics of small tropical cumulus clouds and their impact on the environment, Journal of Geophysical Research: Atmospheres, 103, 28 753–28 767, https://doi.org/10.1029/98JD02579, https://agupubs.onlinelibrary.wiley.com/doi/abs/10.1029/98JD02579, 1998.

Bony, S. and Dufresne, J.-L.: Marine boundary layer clouds at the heart of tropical cloud feedback uncertainties in climate models, Geophysical Research Letters, 32, https://doi.org/10.1029/2005GL023851, https://agupubs.onlinelibrary.wiley.com/doi/abs/10.1029/2005GL023851, 2005.

Boutle, I. A., Abel, S. J., Hill, P. G., and Morcrette, C. J.: Spatial variability of liquid cloud and rain: observations and microphysical effects, Quarterly Journal of the Royal Meteorological Society, 140, 583–594, https://doi.org/10.1002/qj.2140, https://rmets.onlinelibrary.wiley.com/doi/abs/10.1002/qj.2140, 2014.

Bretherton, C. S., McCaa, J. R., and Grenier, H.: A New Parameterization for Shallow Cumulus Convection and Its Application to Marine Subtropical Cloud-Topped Boundary Layers. Part I: Description and 1D Results, Monthly Weather Review, 132, 864–882, https://doi.org/10.1175/1520-0493(2004)132<0864:ANPFSC>2.0.CO;2, https://doi.org/10.1175/1520-0493(2004)132<0864:ANPFSC>2.0.CO;2, 2004.

Burnet, F. and Brenguier, J.-L.: The onset of precipitation in warm cumulus clouds: An observational case-study, Quarterly Journal of the Royal Meteorological Society, pp. n/a–n/a, https://doi.org/10.1002/qj.552, https://doi.org/10.1002%2Fqj.552, 2010.

Chen, B. and Liu, C.: Warm Organized Rain Systems over the Tropical Eastern Pacific, Journal of Climate, 29, 3403–3422, https://doi.org/10.1175/jcli-d-15-0177.1, https://doi.org/10.1175%2Fjcli-d-15-0177.1, 2016.

Christensen, M. W., Stephens, G. L., and Lebsock, M. D.: Exposing biases in retrieved low cloud properties from CloudSat: A guide for evaluating observations and climate data, Journal of Geophysical Research: Atmospheres, 118, 12,120–12,131, https://doi.org/10.1002/2013JD020224, https://agupubs.onlinelibrary.wiley.com/doi/abs/10.1002/2013JD020224, 2013.

Cronk, H. and Partain, P.: CloudSat ECMWF-AUX Auxillary Data Product Process Description and Interface Control Document, Tech. rep., Colorado State University, 2017.

Dagan, G., Koren, I., Altaratz, O., and Heiblum, R. H.: Aerosol effect on the evolution of the thermodynamic properties of warm convective cloud fields, Scientific Reports, 6, https://doi.org/10.1038/srep38769, https://doi.org/10.1038%2Fsrep38769, 2016.

Del Genio, A. D., Kovari, W., Yao, M.-S., and Jonas, J.: Cumulus Microphysics and Climate Sensitivity, Journal of Climate, 18, 2376–2387, https://doi.org/10.1175/JCLI3413.1, https://doi.org/10.1175/JCLI3413.1, 2005.

https://doi.org/10.5194/acp-2020-754
Preprint. Discussion started: 12 August 2020

Dufresne, J.-L. and Bony, S.: An Assessment of the Primary Sources of Spread of Global Warming Estimates from Coupled Atmosphere–Ocean Models, Journal of Climate, 21, 5135–5144, https://doi.org/10.1175/2008JCLI2239.1, https://doi.org/10.1175/2008JCLI2239.1, 2008.

Gerber, H. E., Frick, G. M., Jensen, J. B., and Hudson, J. G.: Entrainment, Mixing, and Microphysics in Trade-Wind Cumulus, Journal of the Meteorological Society of Japan. Ser. II, 86A, 87–106, https://doi.org/10.2151/jmsj.86A.87, 2008.

Hernandez-Deckers, D. and Sherwood, S. C.: On the Role of Entrainment in the Fate of Cumulus Thermals, Journal of the Atmospheric Sciences, 75, 3911–3924, https://doi.org/10.1175/jas-d-18-0077.1, https://doi.org/10.1175%2Fjas-d-18-0077.1, 2018.

Heus, T. and Jonker, H. J. J.: Subsiding Shells around Shallow Cumulus Clouds, Journal of the Atmospheric Sciences, 65, 1003–1018, https://doi.org/10.1175/2007jas2322.1, https://doi.org/10.1175%2F2007jas2322.1, 2008.

Jiang, H. and Feingold, G.: Effect of aerosol on warm convective clouds: Aerosol-cloud-surface flux feedbacks in a new coupled large eddy model, Journal of Geophysical Research: Atmospheres, 111, https://doi.org/10.1029/2005JD006138, https://agupubs.onlinelibrary.wiley.com/doi/abs/10.1029/2005JD006138, 2006.

Jung, E., Albrecht, B. A., Feingold, G., Jonsson, H. H., Chuang, P., and Donaher, S. L.: Aerosols, clouds, and precipitation in the North Atlantic trades observed during the Barbados aerosol cloud experiment – Part 1: Distributions and variability, Atmospheric Chemistry and Physics, 16, 8643–8666, https://doi.org/10.5194/acp-16-8643-2016, https://doi.org/10.5194%2Facp-16-8643-2016, 2016a.

Jung, E., Albrecht, B. A., Sorooshian, A., Zuidema, P., and Jonsson, H. H.: Precipitation susceptibility in marine stratocumulus and shallow cumulus from airborne measurements, Atmospheric Chemistry and Physics, 16, 11 395–11 413, https://doi.org/10.5194/acp-16-11395-2016, https://doi.org/10.5194%2Facp-16-11395-2016, 2016b.

Koren, I., Dagan, G., and Altaratz, O.: From aerosol-limited to invigoration of warm convective clouds, Science, 344, 1143–1146, https://doi.org/10.1126/science.1252595, https://science.sciencemag.org/content/344/6188/1143, 2014.

Korolev, A., Khain, A., Pinsky, M., and French, J.: Theoretical study of mixing in liquid clouds – Part 1: Classical concepts, Atmospheric Chemistry and Physics, 16, 9235–9254, https://doi.org/10.5194/acp-16-9235-2016, https://doi.org/10.5194%2Facp-16-9235-2016, 2016.

Lau, K. M. and Wu, H. T.: Warm rain processes over tropical oceans and climate implications, Geophysical Research Letters, 30, https://doi.org/10.1029/2003GL018567, https://agupubs.onlinelibrary.wiley.com/doi/abs/10.1029/2003GL018567, 2003.

Lebsock, M. and Su, H.: Application of active spaceborne remote sensing for understanding biases between passive cloud water path retrievals, Journal of Geophysical Research: Atmospheres, 119, 8962–8979, https://doi.org/10.1002/2014JD021568, https://agupubs.onlinelibrary.wiley.com/doi/abs/10.1002/2014JD021568, 2014.

Lebsock, M., Morrison, H., and Gettelman, A.: Microphysical implications of cloud-precipitation covariance derived from satellite remote sensing, Journal of Geophysical Research: Atmospheres, 118, 6521–6533, https://doi.org/10.1002/jgrd.50347, https://agupubs.onlinelibrary.wiley.com/doi/abs/10.1002/jgrd.50347, 2013.

Lebsock, M. D. and L'Ecuyer, T. S.: The retrieval of warm rain from CloudSat, Journal of Geophysical Research: Atmospheres, 116, https://doi.org/10.1029/2011JD016076, https://agupubs.onlinelibrary.wiley.com/doi/abs/10.1029/2011JD016076, 2011.

Lebsock, M. D., L'Ecuyer, T. S., and Stephens, G. L.: Detecting the Ratio of Rain and Cloud Water in Low-Latitude Shallow Marine Clouds, Journal of Applied Meteorology and Climatology, 50, 419–432, https://doi.org/10.1175/2010JAMC2494.1, https://doi.org/10.1175/2010JAMC2494.1, 2011.

L'Ecuyer, T. S. and Stephens, G. L.: An Estimation-Based Precipitation Retrieval Algorithm for Attenuating Radars, Journal of Applied Meteorology, 41, 272–285, https://doi.org/10.1175/1520-0450(2002)041<0272:AEBPRA>2.0.CO;2, https://doi.org/10.1175/1520-0450(2002)041<0272:AEBPRA>2.0.CO;2, 2002.

https://doi.org/10.5194/acp-2020-754
Preprint. Discussion started: 12 August 2020

Lee, H. and Baik, J.-J.: A Physically Based Autoconversion Parameterization, Journal of the Atmospheric Sciences, 74, 1599–1616, https://doi.org/10.1175/JAS-D-16-0207.1, https://doi.org/10.1175/JAS-D-16-0207.1, 2017.

Lim, K.-S. S. and Hong, S.-Y.: Development of an Effective Double-Moment Cloud Microphysics Scheme with Prognostic Cloud Condensation Nuclei (CCN) for Weather and Climate Models, Monthly Weather Review, 138, 1587–1612, https://doi.org/10.1175/2009MWR2968.1, https://doi.org/10.1175/2009MWR2968.1, 2010.

Liu, Y. and Daum, P. H.: Parameterization of the Autoconversion Process.Part I: Analytical Formulation of the Kessler-Type Parameterizations, Journal of the Atmospheric Sciences, 61, 1539–1548, https://doi.org/10.1175/1520-0469(2004)061<1539:POTAPI>2.0.CO;2, https://doi.org/10.1175/1520-0469(2004)061<1539:POTAPI>2.0.CO;2, 2004.

Lohmann, U. and Roeckner, E.: Design and performance of a new cloud microphysics scheme developed for the ECHAM general circulation model, Climate Dynamics, 12, 557–572, https://doi.org/10.1007/BF00207939, https://doi.org/10.1007/BF00207939, 1996.

Lu, C., Liu, Y., Niu, S., and Vogelmann, A. M.: Lateral entrainment rate in shallow cumuli: Dependence on dry air sources and probability density functions, Geophysical Research Letters, 39, https://doi.org/10.1029/2012GL053646, https://agupubs.onlinelibrary.wiley.com/doi/abs/10.1029/2012GL053646, 2012.

Lutsko, N. J. and Cronin, T. W.: Increase in Precipitation Efficiency With Surface Warming in Radiative-Convective Equilibrium, Journal of Advances in Modeling Earth Systems, 10, 2992–3010, https://doi.org/10.1029/2018MS001482, https://agupubs.onlinelibrary.wiley.com/doi/abs/10.1029/2018MS001482, 2018.

Marchand, R., Mace, G. G., Ackerman, T., and Stephens, G.: Hydrometeor Detection Using Cloudsat—An Earth-Orbiting 94-GHz Cloud Radar, Journal of Atmospheric and Oceanic Technology, 25, 519–533, https://doi.org/10.1175/2007JTECHA1006.1, https://doi.org/10.1175/2007JTECHA1006.1, 2008.

Medeiros, B. and Stevens, B.: Revealing differences in GCM representations of low clouds, Climate Dynamics, 36, 385–399, https://doi.org/10.1007/s00382-009-0694-5, https://doi.org/10.1007/s00382-009-0694-5, 2011.

Minor, H. A., Rauber, R. M., Göke, S., and Di Girolamo, L.: Trade Wind Cloud Evolution Observed by Polarization Radar: Relationship to Giant Condensation Nuclei Concentrations and Cloud Organization, Journal of the Atmospheric Sciences, 68, 1075–1096, https://doi.org/10.1175/2010JAS3675.1, https://doi.org/10.1175/2010JAS3675.1, 2011.

Mitrescu, C., L'Ecuyer, T., Haynes, J., Miller, S., and Turk, J.: CloudSat Precipitation Profiling Algorithm—Model Description, Journal of Applied Meteorology and Climatology, 49, 991–1003, https://doi.org/10.1175/2009JAMC2181.1, https://doi.org/10.1175/2009JAMC2181.1, 2010.

Morrison, H., Curry, J. A., and Khvorostyanov, V. I.: A New Double-Moment Microphysics Parameterization for Application in Cloud and Climate Models. Part I: Description, Journal of the Atmospheric Sciences, 62, 1665–1677, https://doi.org/10.1175/JAS3446.1, https://doi.org/10.1175/JAS3446.1, 2005.

Moser, D. H. and Lasher-Trapp, S.: The Influence of Successive Thermals on Entrainment and Dilution in a Simulated Cumulus Congestus, Journal of the Atmospheric Sciences, 74, 375–392, https://doi.org/10.1175/JAS-D-16-0144.1, https://doi.org/10.1175/JAS-D-16-0144.1, 2017.

Nam, C., Bony, S., Dufresne, J.-L., and Chepfer, H.: The 'too few, too bright' tropical low-cloud problem in CMIP5 models, Geophysical Research Letters, 39, https://doi.org/10.1029/2012GL053421, https://agupubs.onlinelibrary.wiley.com/doi/abs/10.1029/2012GL053421, 2012.

Pinsky, M., Khain, A., and Korolev, A.: Theoretical analysis of mixing in liquid clouds – Part 3: Inhomogeneous mixing, Atmospheric Chemistry and Physics, 16, 9273–9297, https://doi.org/10.5194/acp-16-9273-2016, https://doi.org/10.5194%2Facp-16-9273-2016, 2016a.

https://doi.org/10.5194/acp-2020-754
Preprint. Discussion started: 12 August 2020

Pinsky, M., Khain, A., Korolev, A., and Magaritz-Ronen, L.: Theoretical investigation of mixing in warm clouds – Part 2: Homogeneous mixing, Atmospheric Chemistry and Physics, 16, 9255–9272, https://doi.org/10.5194/acp-16-9255-2016, https://doi.org/10.5194%2Facp-16-9255-2016, 2016b.

Platnick, S., King, M. D., Ackerman, S. A., Menzel, W. P., Baum, B. A., Riedi, J. C., and Frey, R. A.: The MODIS cloud products: algorithms and examples from Terra, IEEE Transactions on Geoscience and Remote Sensing, 41, 459–473, 2003.

Rauber, R. M., Stevens, B., Ochs, H. T., Knight, C., Albrecht, B. A., Blyth, A. M., Fairall, C. W., Jensen, J. B., Lasher-Trapp, S. G., Mayol-Bracero, O. L., Vali, G., Anderson, J. R., Baker, B. A., Bandy, A. R., Burnet, E., Brenguier, J.-L., Brewer, W. A., Brown, P. R. A., Chuang, R., Cotton, W. R., Girolamo, L. D., Geerts, B., Gerber, H., GÃ¶ke, S., Gomes, L., Heikes, B. G., Hudson, J. G., Kollias, P., Lawson, R. R., Krueger, S. K., Lenschow, D. H., Nuijens, L., O'Sullivan, D. W., Rilling, R. A., Rogers, D. C., Siebesma, A. P., Snodgrass, E., Stith, J. L., Thornton, D. C., Tucker, S., Twohy, C. H., and Zuidema, P.: Rain in Shallow Cumulus Over the Ocean: The RICO Campaign, Bulletin of the American Meteorological Society, 88, 1912–1928, https://doi.org/10.1175/bams-88-12-1912, https://doi.org/10.1175%2Fbams-88-12-1912, 2007.

Rennó, N. O., Emanuel, K. A., and Stone, P. H.: Radiative-convective model with an explicit hydrologic cycle: 1. Formulation and sensitivity to model parameters, Journal of Geophysical Research: Atmospheres, 99, 14 429–14 441, https://doi.org/10.1029/94JD00020, https://agupubs.onlinelibrary.wiley.com/doi/abs/10.1029/94JD00020, 1994.

Romps, D. M.: An Analytical Model for Tropical Relative Humidity, Journal of Climate, 27, 7432–7449, https://doi.org/10.1175/JCLI-D-14-00255.1, https://doi.org/10.1175/JCLI-D-14-00255.1, 2014.

Ruiz-Arias, J. A., Dudhia, J., Gueymard, C. A., and Pozo-Vázquez, D.: Assessment of the Level-3 MODIS daily aerosol optical depth in the context of surface solar radiation and numerical weather modeling, Atmospheric Chemistry and Physics, 13, 675–692, https://doi.org/10.5194/acp-13-675-2013, https://www.atmos-chem-phys.net/13/675/2013/, 2013.

Saleeby, S. M., Herbener, S. R., van den Heever, S. C., and L'Ecuyer, T.: Impacts of Cloud Droplet–Nucleating Aerosols on Shallow Tropical Convection, Journal of the Atmospheric Sciences, 72, 1369–1385, https://doi.org/10.1175/JAS-D-14-0153.1, https://doi.org/10.1175/JAS-D-14-0153.1, 2015.

Schmeissner, T., Shaw, R. A., Ditas, J., Stratmann, F., Wendisch, M., and Siebert, H.: Turbulent Mixing in Shallow Trade Wind Cumuli: Dependence on Cloud Life Cycle, Journal of the Atmospheric Sciences, 72, 1447–1465, https://doi.org/10.1175/jas-d-14-0230.1, https://doi.org/10.1175%2Fjas-d-14-0230.1, 2015.

Short, D. A. and Nakamura, K.: TRMM Radar Observations of Shallow Precipitation over the Tropical Oceans, Journal of Climate, 13, 4107–4124, https://doi.org/10.1175/1520-0442(2000)013<4107:TROOSP>2.0.CO;2, https://doi.org/10.1175/1520-0442(2000)013<4107:TROOSP>2.0.CO;2, 2000.

Smalley, K. M. and Rapp, A. D.: The role of cloud size and environmental moisture in shallow cumulus precipitation, Journal of Applied Meteorology and Climatology, 0, null, https://doi.org/10.1175/JAMC-D-19-0145.1, https://doi.org/10.1175/JAMC-D-19-0145.1, 2020.

Squires, P.: The Microstructure and Colloidal Stability of Warm Clouds, Tellus, 10, 256–261, https://doi.org/10.1111/j.2153-3490.1958.tb02011.x, https://onlinelibrary.wiley.com/doi/abs/10.1111/j.2153-3490.1958.tb02011.x, 1958.

Stevens, D. E., Ackerman, A. S., and Bretherton, C. S.: Effects of domain size and numerical resolution on the simulation of shallow cumulus convection, J. Atmos. Sci., 59, 3285–3301, https://doi.org/10.1175/1520-0469(2002)0593C32853AEODSAN3E2.0.CO;2, 2002.

Tanelli, S., Durden, S. L., Im, E., Pak, K. S., Reinke, D. G., Partain, P., Haynes, J. M., and Marchand, R. T.: CloudSat's Cloud Profiling Radar After Two Years in Orbit: Performance, Calibration, and Processing, IEEE Transactions on Geoscience and Remote Sensing, 46, 3560–3573, https://doi.org/10.1109/TGRS.2008.2002030, 2008.

https://doi.org/10.5194/acp-2020-754
Preprint. Discussion started: 12 August 2020

Tian, Y. and Kuang, Z.: Dependence of entrainment in shallow cumulus convection on vertical velocity and distance to cloud edge, Geophysical Research Letters, 43, 4056–4065, https://doi.org/10.1002/2016gl069005, https://doi.org/10.1002%2F2016gl069005, 2016.

Tiedtke, M.: A Comprehensive Mass Flux Scheme for Cumulus Parameterization in Large-Scale Models, Monthly Weather Review, 117, 1779–1800, https://doi.org/10.1175/1520-0493(1989)117<1779:ACMFSF>2.0.CO;2, https://doi.org/10.1175/1520-0493(1989)117<1779:ACMFSF>2.0.CO;2, 1989.

Trivej, P. and Stevens, B.: The Echo Size Distribution of Precipitating Shallow Cumuli, Journal of the Atmospheric Sciences, 67, 788–804, https://doi.org/10.1175/2009JAS3178.1, https://doi.org/10.1175/2009JAS3178.1, 2010.

Twomey, S.: Pollution and the planetary albedo, Atmospheric Environment, 8, 1251 – 1256, https://doi.org/https://doi.org/10.1016/0004-6981(74)90004-3, http://www.sciencedirect.com/science/article/pii/0004698174900043, 1974.

Vial, J., Dufresne, J.-L., and Bony, S.: On the interpretation of inter-model spread in CMIP5 climate sensitivity estimates, Climate Dynamics, 41, 3339–3362, https://doi.org/10.1007/s00382-013-1725-9, https://doi.org/10.1007/s00382-013-1725-9, 2013.

Waliser, D. E. and Gautier, C.: A Satellite-derived Climatology of the ITCZ, Journal of Climate, 6, 2162–2174, https://doi.org/10.1175/1520-0442(1993)006<2162:ASDCOT>2.0.CO;2, https://doi.org/10.1175/1520-0442(1993)006<2162:ASDCOT>2.0.CO;2, 1993.

Wang, Y., Chen, Y., Fu, Y., and Liu, G.: Identification of precipitation onset based on Cloudsat observations, Journal of Quantitative Spectroscopy and Radiative Transfer, 188, 142 – 147, https://doi.org/https://doi.org/10.1016/j.jqsrt.2016.06.028, http://www.sciencedirect.com/science/article/pii/S0022407315301886, advances in Atmospheric Light Scattering: Theory and Remote Sensing Techniques, 2017.

Witkowski, M., Vane, D., Livermore, T., Rokey, M., Barthuli, M., Gravseth, I. J., Pieper, B., Rodzinak, A., Silva, S., and Woznick, P.: CloudSat anomaly recovery and operational lessons learned, Tech. rep., Jet Propulsion Laboratory, National Aeronautics and Space Administration, 2012.

Witte, M. K., Morrison, H., Jensen, J. B., Bansemer, A., and Gettelman, A.: On the Covariability of Cloud and Rain Water as a Function of Length Scale, Journal of the Atmospheric Sciences, 76, 2295–2308, https://doi.org/10.1175/JAS-D-19-0048.1, https://doi.org/10.1175/JAS-D-19-0048.1, 2019.

Wood, R. and Bretherton, C. S.: Boundary Layer Depth, Entrainment, and Decoupling in the Cloud-Capped Subtropical and Tropical Marine Boundary Layer, Journal of Climate, 17, 3576–3588, https://doi.org/10.1175/1520-0442(2004)017<3576:BLDEAD>2.0.CO;2, https://doi.org/10.1175/1520-0442(2004)017<3576:BLDEAD>2.0.CO;2, 2004a.

Wood, R. and Bretherton, C. S.: Boundary Layer Depth, Entrainment, and Decoupling in the Cloud-Capped Subtropical and Tropical Marine Boundary Layer, Journal of Climate, 17, 3576–3588, https://doi.org/10.1175/1520-0442(2004)017<3576:BLDEAD>2.0.CO;2, https://doi.org/10.1175/1520-0442(2004)017<3576:BLDEAD>2.0.CO;2, 2004b.

Wyant, M. C., Khairoutdinov, M., and Bretherton, C. S.: Climate sensitivity and cloud response of a GCM with a superparameterization, Geophysical Research Letters, 33, https://doi.org/10.1029/2005GL025464, https://agupubs.onlinelibrary.wiley.com/doi/abs/10.1029/2005GL025464, 2006.

Zhang, G. and McFarlane, N. A.: Sensitivity of climate simulations to the parameterization of cumulus convection in the Canadian climate centre general circulation model, Atmosphere-Ocean, 33, 407–446, https://doi.org/10.1080/07055900.1995.9649539, https://doi.org/10.1080/07055900.1995.9649539, 1995.

Zhao, M.: An Investigation of the Connections among Convection, Clouds, and Climate Sensitivity in a Global Climate Model, Journal of Climate, 27, 1845–1862, https://doi.org/10.1175/JCLI-D-13-00145.1, https://doi.org/10.1175/JCLI-D-13-00145.1, 2014.

https://doi.org/10.5194/acp-2020-754
Preprint. Discussion started: 12 August 2020

Atmospheric Chemistry and Physics Discussions
Open Access
EGU

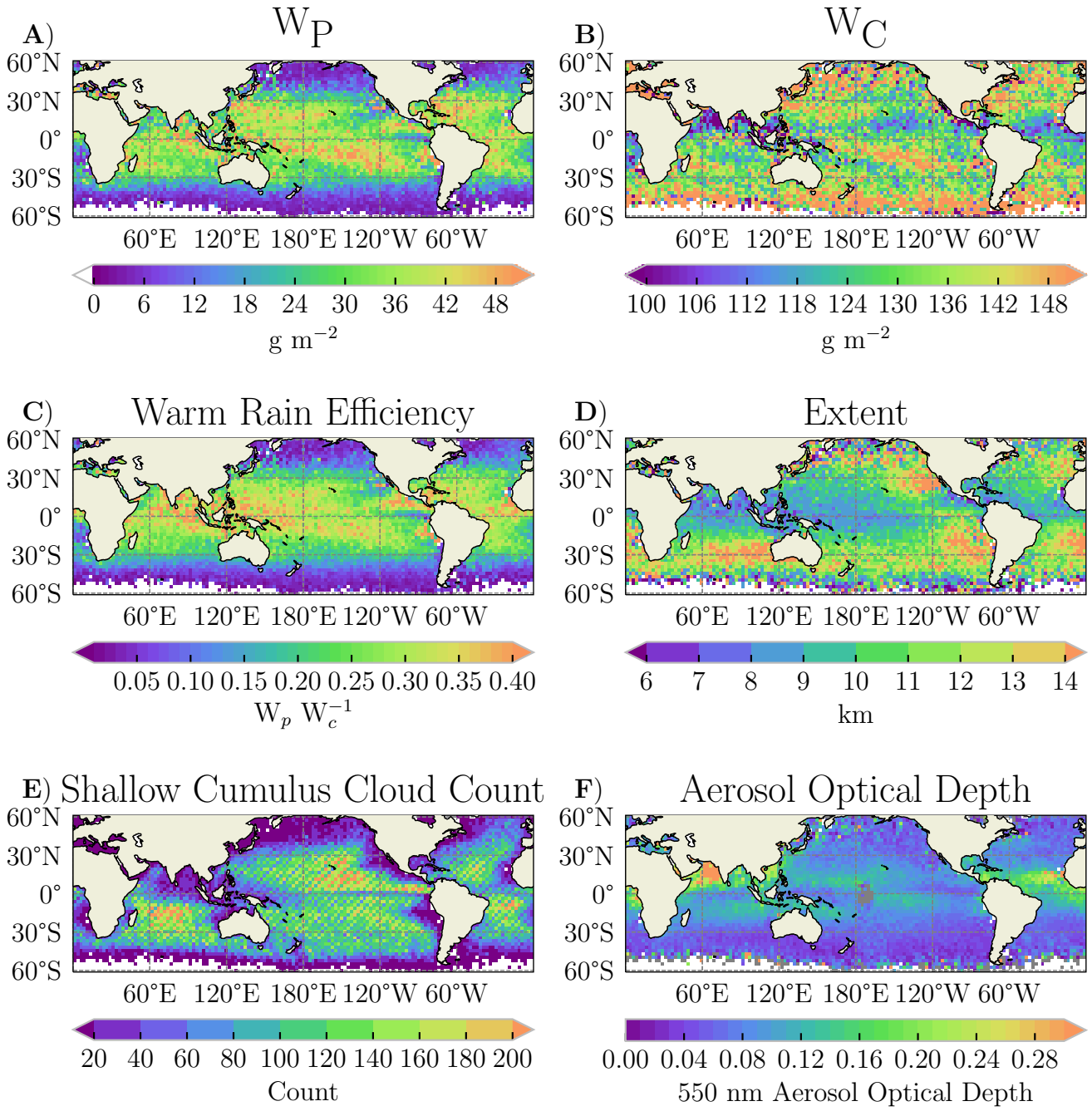

Figure 1. The spatial distribution of integrated precipitation water path (W_P), cloud water path (W_C), warm rain efficiency, extent, number of shallow cumulus cloud objects, and aerosol optical depth are shown in panels A), B), C), D), E), and F) respectively. Cloud objects are binned onto a 2.5° x 2.5° spatial grid, and any grid box containing no data is white.

https://doi.org/10.5194/acp-2020-754
Preprint. Discussion started: 12 August 2020

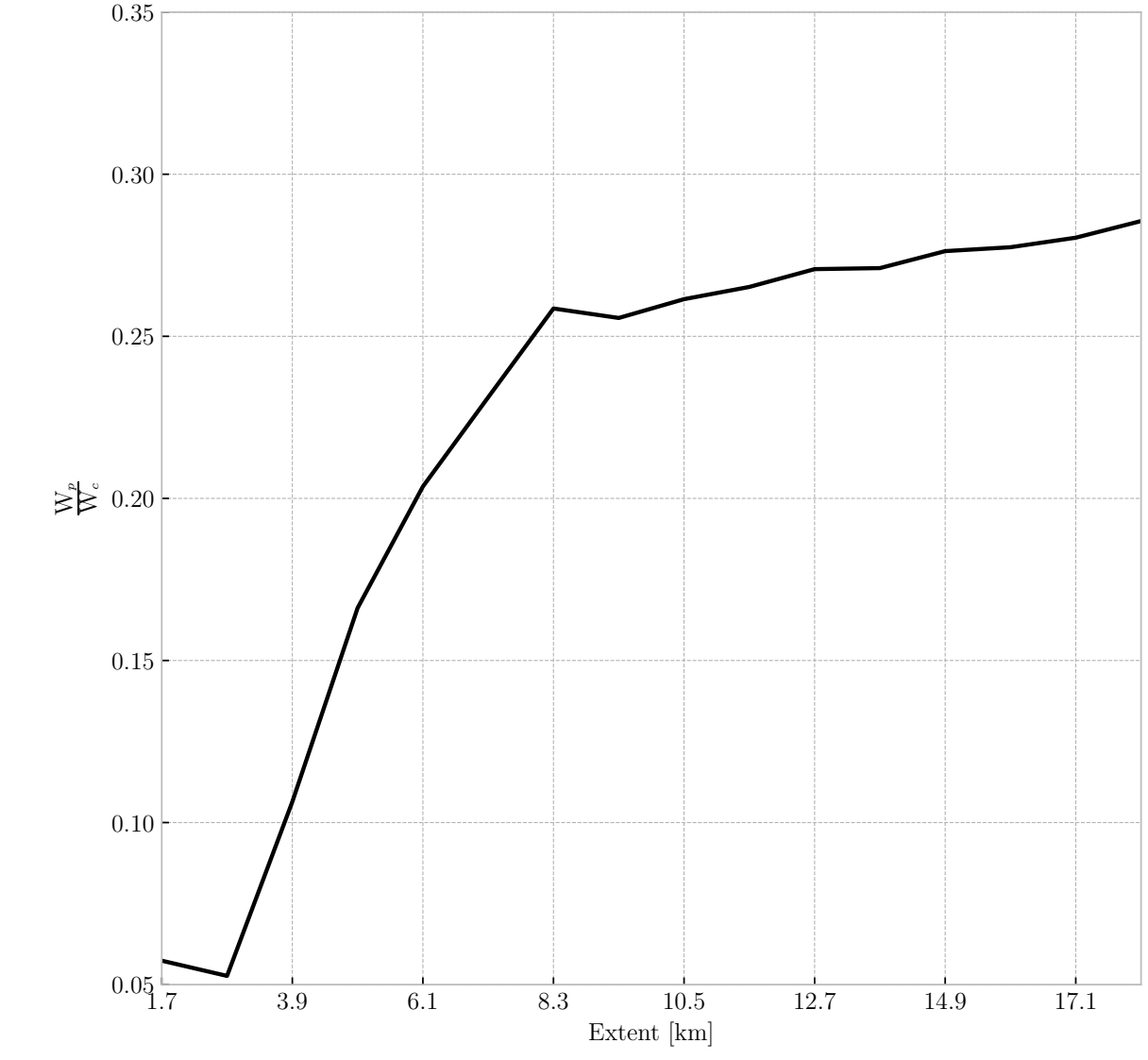

Figure 2. The median warm rain efficiency $\left(\frac{W_p}{W_c}\right)$ at a given median size (extent).

https://doi.org/10.5194/acp-2020-754
Preprint. Discussion started: 12 August 2020

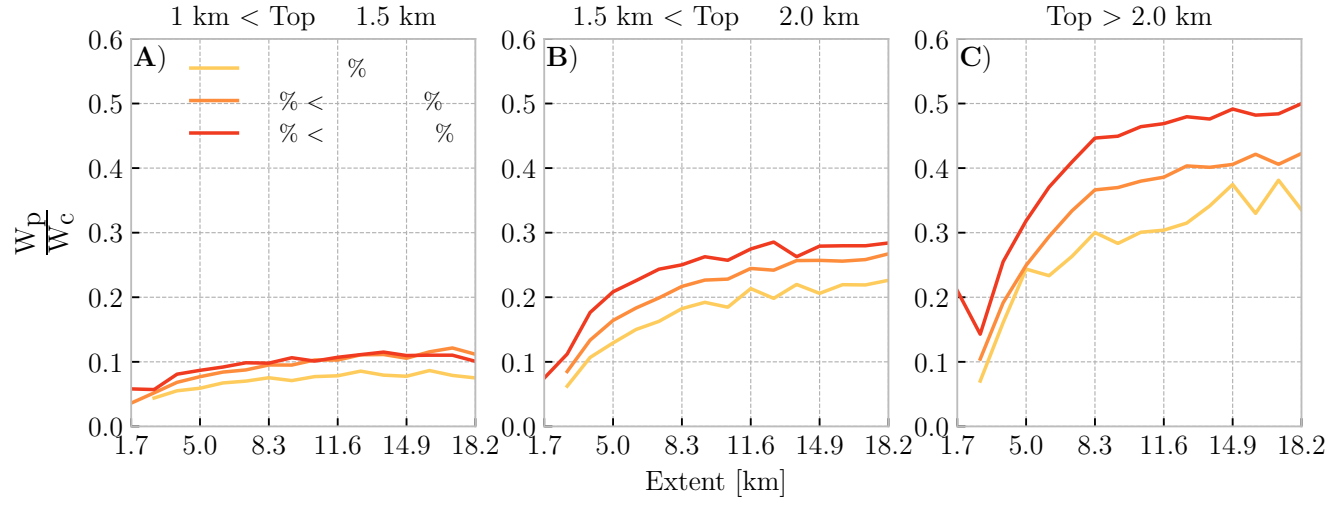

Figure 3. The median warm rain efficiency $\left(\frac{W_p}{W_c}\right)$ at a given median size (extent). The different line colors represent cloud objects separated by environmental moisture (< 3 km relative humidity).

https://doi.org/10.5194/acp-2020-754
Preprint. Discussion started: 12 August 2020

Atmospheric Chemistry and Physics Discussions

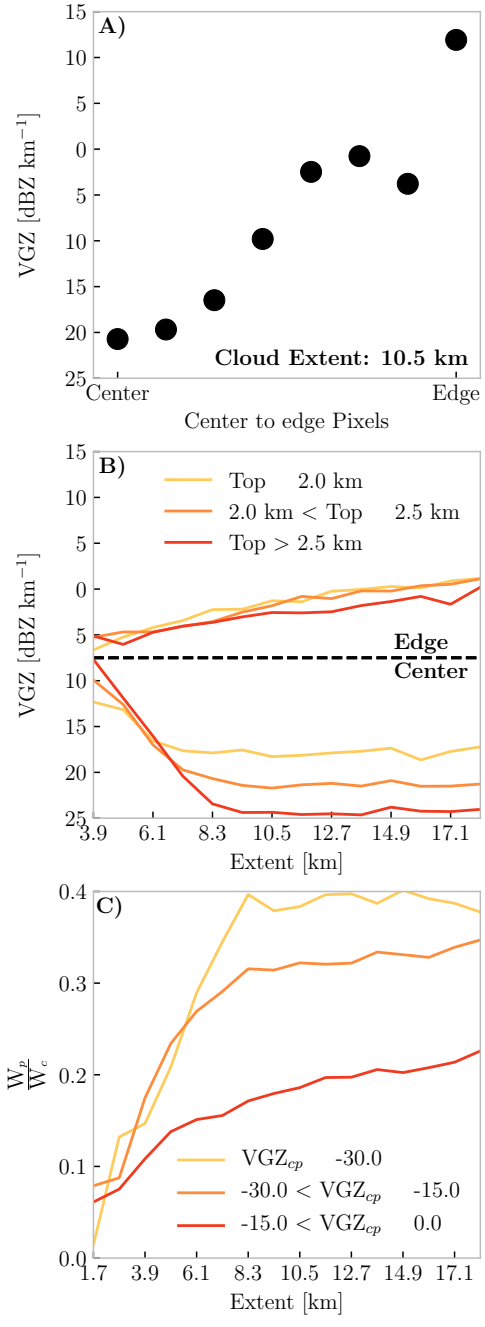

Figure 4. Panel A) shows the median change in the vertical reflectivity (VGZ) from the center to edge of all cloud objects with an extent of 10.5 km. Panel B) shows the median vertical reflectivity gradient (VGZ) at the center (red) and edge (blue) of different sized (extent) raining cloud objects. Different lines represent cloud objects separated by top height. Panel C) shows the median warm rain efficiency ($\frac{W_P}{W_C}$) at a given median size (extent). The different line colors represent cloud objects separated by the vertical reflectivity gradient on the center pixel (VGZ_{cp}) of all cloud objects.

https://doi.org/10.5194/acp-2020-754
Preprint. Discussion started: 12 August 2020

Atmospheric Chemistry and Physics Discussions

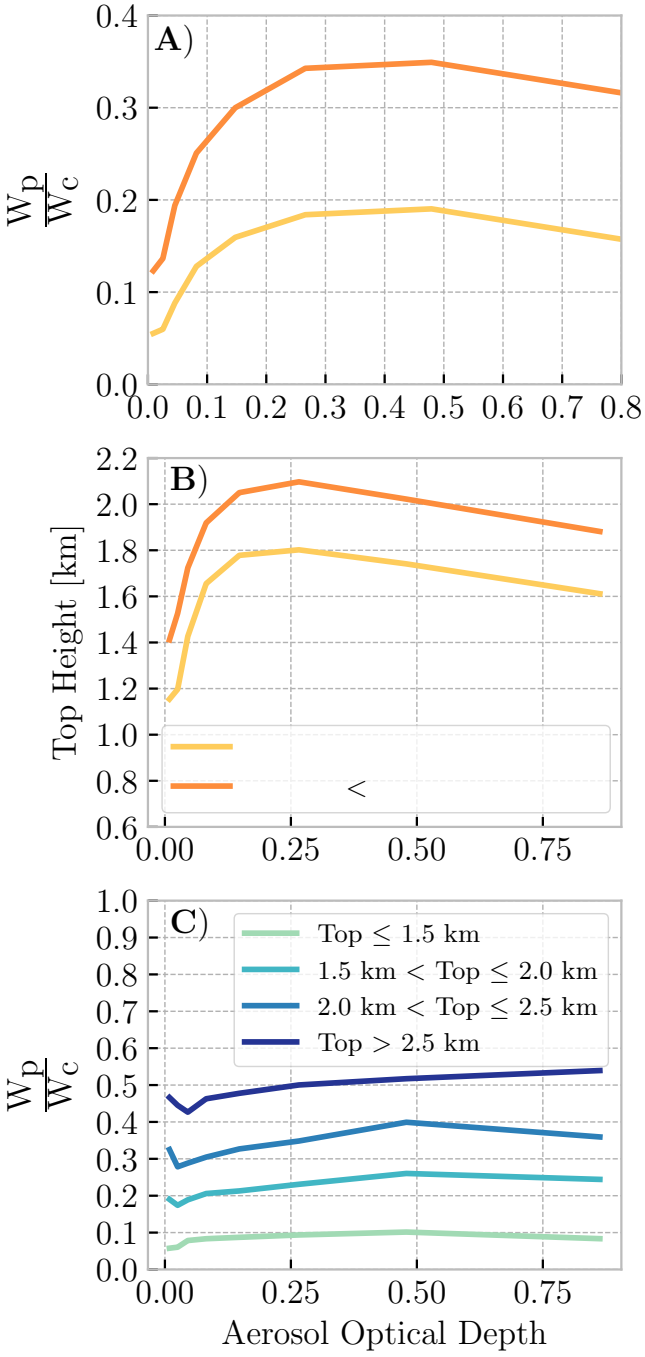

Figure 5. Panel A) shows the relationship between median warm rain efficiency as MODIS 550 nm aerosol optical depth. Panel B) shows the relationship between median cloud-top height and aerosol optical depth. Panel C) shows the relationship between warm rain efficiency $\left(\frac{W_p}{W_c}\right)$ and aerosol optical depth. Line colors in panels A) and B) represent cloud objects separated by extent, while line colors in panel C) represent cloud objects separated by top height.

https://doi.org/10.5194/acp-2020-754
Preprint. Discussion started: 12 August 2020

Atmospheric Chemistry and Physics Discussions

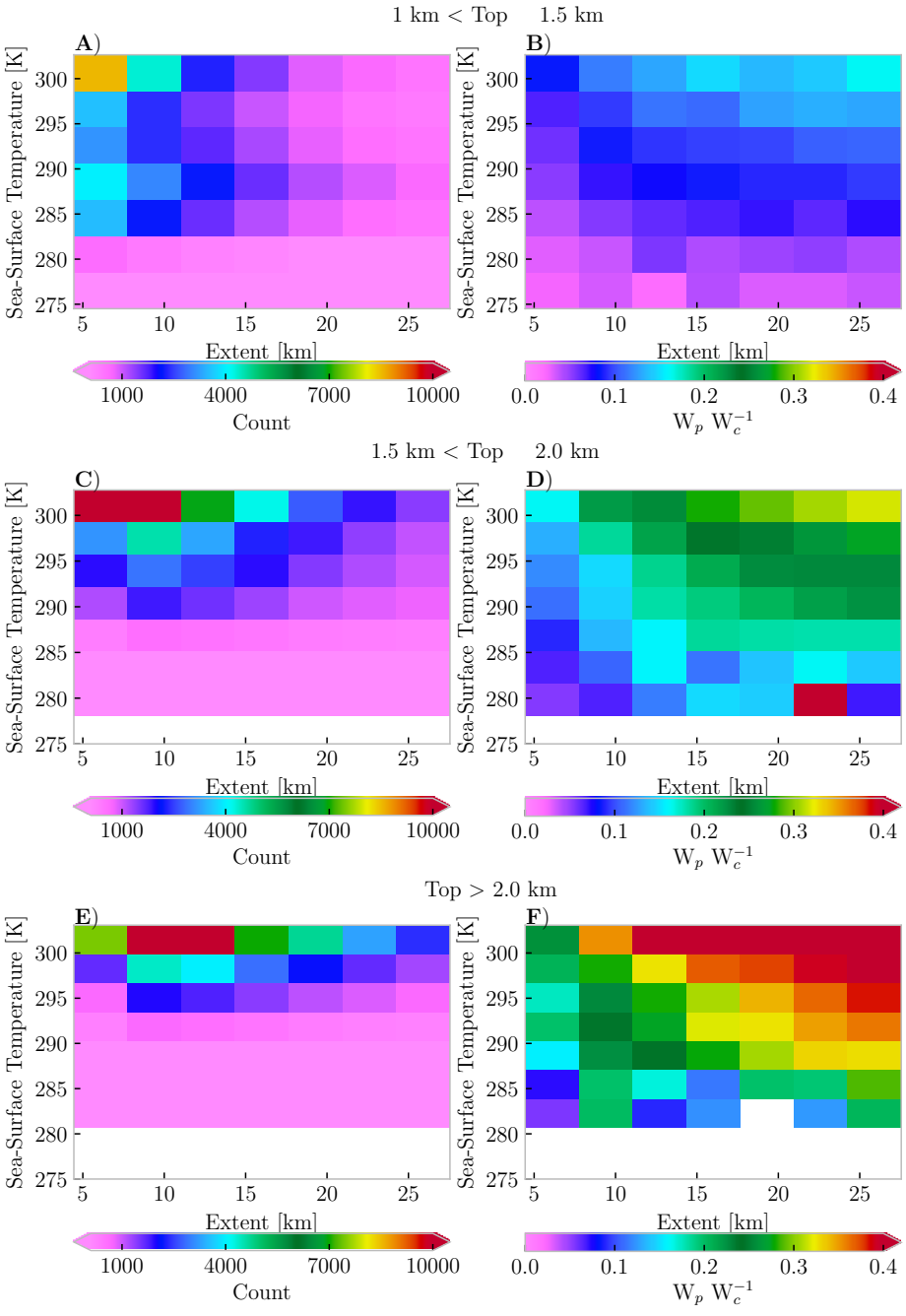

Figure 6. The two-dimensional distribution of extent as a function of sea-surface temperature, conditioned by cloud-top height, is shown in panels A), C), and E) respectively. The median warm rain efficiency (W_p W_c^{-1}) as a function of Extent and sea-surface temperature are shown in panels B), D), and F) respectively.